

Concentration inhomogeneities in random magnets. II. Effects on critical-phenomena studies

D. P. Belanger

Department of Physics, University of California, Santa Cruz, California 95064

A. R. King, I. B. Ferreira, and V. Jaccarino

Department of Physics, University of California, Santa Barbara, California 93106

(Received 9 March 1987)

The effects that concentration inhomogeneities in two-component magnetic systems have on the critical behavior at the second-order phase transition T_N are explicitly determined. Use is made of the technique developed in the preceding paper (I) to first properly characterize the concentration variation $x(\mathbf{r})$ as a function of position \mathbf{r} in a prototype diluted Ising antiferromagnet, $\text{Fe}_x\text{Zn}_{1-x}\text{F}_2$. Then, with the known dependence of $T_N(x)$ on x , simulations are made of the magnetic specific-heat anomaly and the quasielastic-neutron-scattering line profile as a function of reduced temperature for the random-exchange Ising-model system. The simulations reproduce experimental measurements on systems with predetermined linear concentration gradients. Errors in crossover and critical exponents in studies by others of the phase transition region in random magnets are shown to result from neglect or improper treatment of concentration gradient effects on critical behavior. It is argued that different distribution functions for concentration gradients, with the same variance, will lead to different effective critical behavior; hence knowing the latter is not sufficient in predicting the former. This is exemplified in an analysis of a neutron-scattering experiment whose critical behavior *cannot* be fitted by any choice of assumed *linear* gradient.

I. INTRODUCTION

In the preceding paper¹ (hereafter referred to as I) we have demonstrated that the macroscopic concentration gradient in a particular two-component system $\text{Fe}_x\text{Zn}_{1-x}\text{F}_2$, can be precisely determined using the optical birefringence (Δn) technique. Since the magnetic ordering temperature T_N of a randomly diluted antiferromagnet such as $\text{Fe}_x\text{Zn}_{1-x}\text{F}_2$ varies with the concentration x in a known way,² it follows that one would expect to be able to simulate the critical behavior of the system, once the concentration distribution is given. (This assumes the relevant critical exponents and amplitude ratios are known.) We justify a procedure for doing just that below. We give examples of simulations that have been made of thermodynamic functions on crystals whose gradients have been measured by the method described in I, and compare the results of the simulations with the observed critical behavior. The logic of following this sequence—first determining the spatial variation in concentration and then using this knowledge to simulate the critical phenomena—seems patently obvious. Nevertheless, almost without exception, the exact opposite sequence has been followed in many studies of critical behavior in random systems; namely that of trying to judge the concentration variation from the apparent rounding of the phase transition.^{3–5}

The reason for following this latter course is one of expedience. Most critical phenomena experimentalists do not have ready access to a nondestructive technique for performing the requisite concentration variation analysis in random systems. In some instances, a slice is

taken from either end of the crystal to be studied and a chemical analysis is made to estimate an upper limit on the average gradient. As is seen in Fig. 7 of I, this procedure is fraught with danger.

We show that the true critical behavior is observed only well outside the region of rounding caused by concentration gradients, and therefore one must restrict the analysis of critical behavior to well outside that region. Furthermore, we show, in a particular instance, that the form of the rounded data is particularly insensitive to the values of the critical exponents, and that it is thus impossible to extract exponents from the data in the region of rounding. Even if one is only interested in the general character of the phase transition and not the detailed critical behavior, gradient-induced rounding, if not independently known, can lead to incorrect conclusions about the sharpness (and possibly the *order*) of the transition.

II. ASSUMPTIONS UNDERLYING SIMULATIONS OF OBSERVED CRITICAL BEHAVIOR IN THE PRESENCE OF CONCENTRATION INHOMOGENEITIES

Once having established the nature of the macroscopic inhomogeneity of the distribution of magnetic ions, one must next consider the effect that this particular kind of nonrandomness has on the observed critical phenomena. Various theoretical models of deviations from microscopic randomness have been put forth and their consequences on critical phenomena analyzed.⁶ None are specific to the concentration gradient type of macroscop-

ic inhomogeneity, but some of the considerations underlying these models do have some bearing on the problem at hand.

The existence of a concentration gradient large enough so that the fractional variation in T_c over the sample would be, say $\delta T_c/T_c \geq 10^{-3}$, intuitively suggests that rounding of the phase transition to this degree would be observed in all measured critical phenomena. The question is—how can one quantify these expectations? We propose to analyze the observed behavior of systems with short-range interaction in terms of a model which assumes that there is a one-to-one correspondence between the local concentration $x(\mathbf{r})$ and the value of $T_c[x(\mathbf{r})]$ at the point \mathbf{r} . In effect, one presumes there is *no* means by which the spins are forced to undergo a single collective phase transition over some large region of volume V (of order of a sizeable fraction of the sample) at a temperature

$$\bar{T}_c = \frac{1}{V} \int_V T_c[x(\mathbf{r})] dV. \quad (1)$$

The justification for this simplest of all approaches can be found, for example, in a model of Föhnle⁶ in which he considered an array of small interacting ferromagnetic grains each of volume V with a well-defined T_c . T_c varies in random fashion from grain to grain, with a dispersion in the local *reduced* temperature t_i of each grain

$$\Delta^2 = \langle t_i^2 \rangle - \langle t_i \rangle^2. \quad (2)$$

One can then show that the reduced temperature region t^* below which the ensemble of grains would exhibit critical behavior identical to that of a *homogeneous* system is given by

$$t^* \simeq (V \Delta^2 / \xi_0^d)^{1/\alpha}, \quad (3)$$

where ξ_0 is the amplitude of the critical divergence of the correlation length ($\xi = \xi_0 |t|^{-\nu}$), d is the space dimension, and α is the specific-heat critical exponent ($C = A |t|^{-\alpha}$). (The further requirement that $\alpha < 0$ for there to be a sharp phase transition is consistent with the Harris criterion⁷). Roughly speaking, $\xi_0 \simeq a_0$, the magnetic lattice spacing, so that $V/\xi_0^d \simeq N_v$, the number of spins in the volume V . Since $1/\alpha \sim -10$ for either the pure $d=3$ Heisenberg or $d=3$ random-exchange Ising models, one sees from Eq. (3) that $N_v \Delta^2 < 3$ for $t^* > 10^{-5}$. Neglecting the factor of 3, one might simply say N_v not exceed the reciprocal of the dispersion for there to be an experimentally accessible critical region.

It is not obvious that one can directly apply Föhnle's analysis to the concentration gradient situation for which the variation in T_c is *not* a statistically random grouping of regions, each with a given T_c . However, it is clear that if the fluctuations in concentration were of a statistical nature and were such as to produce a value of $(\Delta^2)^{1/2} \simeq 10^{-3}$ from the one region to another, Föhnle's argument would require the individual regions to have no more than $\sim 10^6$ spins (for $t^* > 10^{-5}$), a truly micro-

scopic number when compared with the total number of spins even in a small crystal: $N \simeq 10^{20}$. Hence, whether one treats T_c as varying on a microscopic scale as a function of position or as an average over regions of order $\Delta^{-2} \xi_0^3$ in size, it matters little when it comes to simulating the critical behavior in crystals of truly macroscopic dimensions, i.e., $V \geq 50 \text{ mm}^3$. Thus in the simulations to follow we will, in the same manner, assume T_c to be a point function of the concentration x and presume (following the method discussed in I) that one can determine x as a function of \mathbf{r} .

We note, however, that the resolution of the techniques of I are at best the width of the laser beam (175 μm), and are thus macroscopic on the scale of correlation lengths at any accessible reduced temperature. Other than truly statistical fluctuations and chemical short-range order, which occurs on atomic length scales and does not therefore limit critical phenomena, the only concentration variations to be expected in the growth process are the gradients discussed in I.

III. SIMULATIONS OF EFFECTS OF CONCENTRATION INHOMOGENEITIES ON CRITICAL BEHAVIOR AND COMPARISONS WITH EXPERIMENT

A. Specific heat $C(T)$

If we assume, as argued in the preceding section, that a one-to-one correspondence exists between the local T_c and the local value of x , we may simulate the effect of the smearing of the phase transition on a particular thermodynamic function simply by convoluting the (known) behavior in the absence of a gradient with the distribution function of transition temperatures; this takes the form of

$$C(T) = \int dT_c W(T_c) [A' |(T - T_c)/T_c|^{-\alpha} H(T - T_c) + A |(T - T_c)/T_c|^{-\alpha} H(T_c - T)]. \quad (4)$$

Here we have chosen the specific heat $C(T)$ as an example, but any other simple thermodynamic function [e.g., susceptibility $\chi(T)$] could be treated in the same way, with appropriate changes of exponents and amplitudes. $W(T_c)$ is the normalized distribution function of T_c , A and A' are the amplitudes above and below T_c , respectively, α is the specific-heat exponent, and $H(x)$ is the Heaviside unit function.

While complex forms for $W(T_c)$ may be found in practice, a particularly simple one is a good representation of a not uncommon form; namely, that of a concentration gradient that leads to a linear variation of T_c with distance r . Assuming such a variation of T_c , with $T_a \leq T_c \leq T_b$, along a sample of uniform cross section, then $W(T_c)$ is given simply by $1/(T_b - T_a)$ for $T_a \leq T_c \leq T_b$, and by zero otherwise. In this case, with $T_b - T_a \ll (T_b + T_a)/2 \equiv \bar{T}_c$, Eq. (4) reduces to

$$C(T) = \begin{cases} A'[(T_b - T)^{1-\alpha} - (T_a - T)^{1-\alpha}] / [(T_b - T_a)(1-\alpha)\bar{T}_c] & \text{for } T \leq T_a, \\ A(T - T_a)^{1-\alpha} + A'(T_b - T)^{1-\alpha} / [(T_b - T_a)(1-\alpha)\bar{T}_c] & \text{for } T_a \leq T \leq T_b, \\ A[(T - T_a)^{1-\alpha} - (T - T_b)^{1-\alpha}] / [(T_b - T_a)(1-\alpha)\bar{T}_c] & \text{for } T \geq T_b, \end{cases} \quad (5a)$$

$$C(T) = \begin{cases} A'[(T_b - T)^{1-\alpha} - (T_a - T)^{1-\alpha}] / [(T_b - T_a)(1-\alpha)\bar{T}_c] & \text{for } T \leq T_a, \\ A(T - T_a)^{1-\alpha} + A'(T_b - T)^{1-\alpha} / [(T_b - T_a)(1-\alpha)\bar{T}_c] & \text{for } T_a \leq T \leq T_b, \\ A[(T - T_a)^{1-\alpha} - (T - T_b)^{1-\alpha}] / [(T_b - T_a)(1-\alpha)\bar{T}_c] & \text{for } T \geq T_b, \end{cases} \quad (5b)$$

$$C(T) = \begin{cases} A'[(T_b - T)^{1-\alpha} - (T_a - T)^{1-\alpha}] / [(T_b - T_a)(1-\alpha)\bar{T}_c] & \text{for } T \leq T_a, \\ A(T - T_a)^{1-\alpha} + A'(T_b - T)^{1-\alpha} / [(T_b - T_a)(1-\alpha)\bar{T}_c] & \text{for } T_a \leq T \leq T_b, \\ A[(T - T_a)^{1-\alpha} - (T - T_b)^{1-\alpha}] / [(T_b - T_a)(1-\alpha)\bar{T}_c] & \text{for } T \geq T_b, \end{cases} \quad (5c)$$

This function is illustrated in Fig. 1. We choose to plot the quantity $d(\Delta n)/dT$ versus T ,⁸ rather than $C(T)$ versus T because we wish to make a comparison later on with birefringence measurements of a diluted antiferromagnet for which $\bar{T}_N = 68.6$ K. $d(\Delta n)/dT$ versus T is shown for two choices of $\delta T_N = T_b - T_a$ along with the case where $\delta T_N = 0$, i.e., when no inhomogeneity is present. The parameters are chosen to approximately correspond to the $d = 3$ random-exchange Ising model (REIM); namely, $\alpha = -0.1$ and $A/A' = 1.6$. We choose \bar{T}_N to be unshifted. T_N lies in a region of negative curvature between T_a and T_b , where sharp changes of slope occur. What is most important is that the peak in $d(\Delta n)/dT$ now lies at T_a , not \bar{T}_N . \bar{T}_N is shifted with respect to the peak by half the extent of the spread of transition temperature.

To test the sensitivity of the shape of the inhomogeneously broadened $d(\Delta n)/dT$ to the parameters appropriate to $d(\Delta n)/dT$ in the absence of such broadening, we have repeated the same simulation but with the parameters of the pure $d = 3$ Ising model; namely, $\alpha = +0.11$ and $A/A' = 0.54$. Remarkably, the new $d(\Delta n)/dT$ -versus- T plot looks very similar to the one obtained with

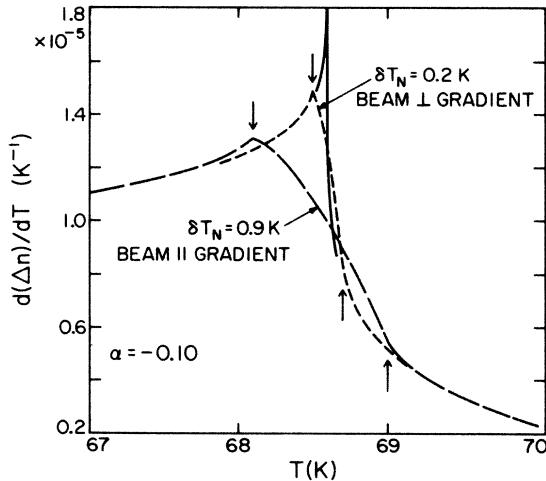


FIG. 1. Simulations of the $d(\Delta n)/dT$ critical behavior $d(\Delta n)/dT = A^\pm |t|^{-\alpha}$ using Eq. (5), with REIM parameters, in the presence of linear concentration gradients. The solid curve is for no gradient with the Néel temperature $T_N = 68.6$ K. The two curves consisting of short or long dashes correspond to $\delta T_N = 0.2$ and 0.9 K, respectively. The arrows indicate the limits of these variations. The average transition temperatures \bar{T}_N are equal to the T_N of the solid curve. Note that the peaks occur at the lower limit of δT_N ; i.e., $\bar{T}_N - \delta T_N/2$, not at \bar{T}_N . The amplitude and the gradients used in this variation correspond to those observed in the sample $\text{Fe}_{0.8}\text{Zn}_{0.2}\text{F}_2$ as is discussed in the text and Figs. 2 and 3.

$\alpha = -0.1$ and $A/A' = 1.6$, even though the REIM case has a cusp and the pure Ising case has a divergence in $d(\Delta n)/dT$. That is to say, the broadened $d(\Delta n)/dT$ for $T_a \leq T \leq T_b$ with pure Ising parameters is practically indistinguishable from the REIM case, having the same general shape and differing from it by at most a few percent. The similarity of the simulations for $\alpha > 0$ and $\alpha < 0$ indicates that this is a general property of any asymmetric function: that \bar{T}_N lies not at the peak, but is displaced toward the steep side of the function.

In both REIM and pure Ising cases, we notice that the broadened $d(\Delta n)/dT$ plots and the unbroadened (no gradient) ones are again indistinguishable when T is only slightly outside the range of the inhomogeneity in T_N , and certainly when T departs from \bar{T}_N by more than δT_N on either side of \bar{T}_N , i.e., $|T - \bar{T}_N| > \delta T_N = T_b - T_a$.

To demonstrate that these calculations correspond to a realistic physical situation, we have performed a test Δn experiment. A sample of a mixed antiferromagnet with nominal composition $\text{Fe}_{0.8}\text{Zn}_{0.2}\text{F}_2$ was selected with a known, rather large, and nearly linear concentration gradient.¹ From room-temperature scans of Δn versus position along the growth axis, illustrated in Fig. 2, and $d(\Delta n)/dx$ from Fig. 2 of I, the overall spread in concentration was determined from Eq. (1) of I to be $\delta x = 1.1\%$ or $\delta x/\delta l = 1.5\% \text{ cm}^{-1}$. This translates into a variation of its Néel temperature $\delta T_N = 0.9$ K, as a consequence of the fact that for $\text{Fe}_x\text{Zn}_{1-x}\text{F}_2$, $T_N(x) = xT_N(1)$ (Ref. 2) for $1 \geq x \geq 0.3$. From scans perpendicular to the growth axis, also illustrated in Fig. 2, we see most of the crystal

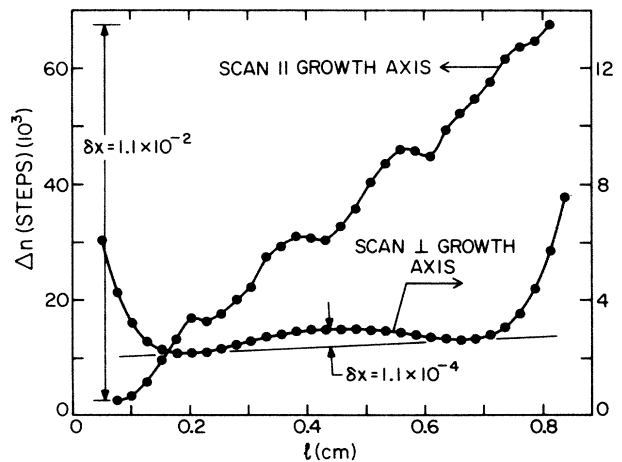


FIG. 2. Birefringence (Δn) scans of the gradient of concentration parallel (\parallel) and perpendicular (\perp) to the crystal growth axis of a particular sample with nominal concentration $\text{Fe}_{0.8}\text{Zn}_{0.2}\text{F}_2$ for which $\bar{T}_N = 68.6$ K. The concentration variation δx in both directions is indicated.

to be uniform in this direction to within $\delta x \sim 10^{-4}$, except for the edges, which show much larger changes over a small region.

We use the now well-established fact that near the phase transition, $d(\Delta n)/dT \sim C(T)$.⁸ To ensure that the $d(\Delta n)/dT$ -versus- T experiment suffered the maximum possible broadening effect from the concentration gradient, we first aligned the laser beam to traverse the sample *parallel* to the growth direction. In this configuration, $d(\Delta n)/dT$ is averaged over the entire concentration variation (and hence the entire T_N variation) from one end of the sample to the other.

The observed $d(\Delta n)/dT$ -versus- T result is shown in Fig. 3 by the open circles. We find a very much broadened transition with a shape almost exactly as predicted in the simulation analysis above: a small peak with a region of negative curvature corresponding to the range of temperatures over which T_N is spread. The line through the data is the simulation of Eqs. (5a)–(5c), with parameters, as in Fig. 1, appropriate to the REIM: $\alpha = -0.10$, $A/A' = 1.6$. The width $T_b - T_a$ has been chosen to equal that determined by the concentration variation: $\delta T_N = 0.9$ K. Only \bar{T}_N and the amplitude have been scaled to fit the data; there are no other adjustable parameters. The agreement between experiment and theory is seen to be excellent.

One of the advantages of $d(\Delta n)/dT$ versus T over the conventional C -versus- T experiment is that one may *minimize* the effects of concentration gradients by aligning the laser beam *perpendicular* to the growth direction, thus sampling the minimum concentration variation.^{9,10} This experiment was also performed on the same $\text{Fe}_{0.80}\text{Zn}_{0.20}\text{F}_2$ crystal but with the laser beam traversing the sample approximately at its midpoint so that $T_N \approx \bar{T}_N$: the results are illustrated in Fig. 3 by the solid dots. The effect of the spread in transition temperatures is seen to be much less than one obtains when the beam is along the gradient. Also, T_N in this case is seen to be close to the midpoint of the region of spread with the beam along the gradient, confirming that \bar{T}_N is indeed in

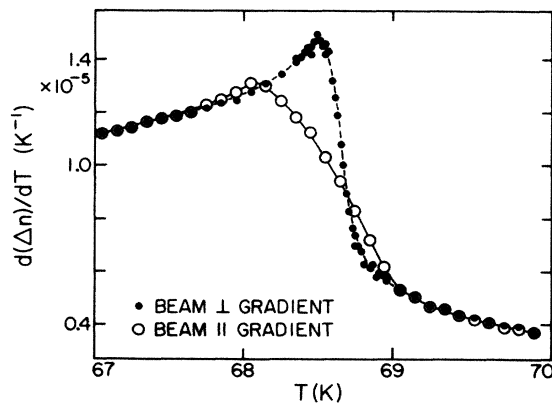


FIG. 3. The observed behavior of $d(\Delta n)/dT$ vs T in the critical region, with the laser beam parallel (open circles) and perpendicular (solid circles) to growth direction, for the $\text{Fe}_{0.8}\text{Zn}_{0.2}\text{F}_2$ crystal whose gradient is shown in Fig. 2. The solid and dashed lines are the respective simulations of Fig. 1 using Eqs. (5a)–(5c). See discussion in text.

this region. Although the concentration variation is not expected to be linear in the direction perpendicular to the growth axis, the form of Eqs. (5a)–(5c) was used to fit the data, with a width $\delta T_N \sim 0.2$ K, resulting in a quite satisfactory fit to the data.

Since one expects a power-law dependence to the critical behavior, it is useful to plot C or $d(\Delta n)/dT$ versus $\log_{10} |t|$. This is done in Fig. 4 for the simulated data of Fig. 1 for the case where $\delta T_N = 0.9$ K. In semilog plots of this type, a weak cusp (small negative α) appears as two lines of slight downward curvature for $t > 0$ and $t < 0$. This intrinsic behavior is indicated in Fig. 4 by the solid lines. When the reduced temperature is defined with respect to \bar{T}_N , i.e., $t = (T - \bar{T}_N)/\bar{T}_N$, the results in the presence of a gradient are affected only slightly for $T < T_a$ and $T > T_b$ (i.e., $|t| > \delta T_N/\bar{T}_N$). However, for $T_a < T < T_c$ (i.e., $|t| < \delta T_N/2\bar{T}_N$), there is an abrupt departure from intrinsic behavior, and the $t > 0$ and $t < 0$ curves meet somewhere between the two intrinsic curves, at a value of $d(\Delta n)/dT$ appropriate to \bar{T}_N .

If t were to be defined with respect to the *peak* in $d(\Delta n)/dT$ at T_a , however, the result would be as shown in Fig. 4 as the short-dashed lines. Although the data for $t < 0$ appears to follow the intrinsic behavior more closely for somewhat smaller $|t|$ than in the previous case, the data for $t > 0$ departs from it at a much larger value of $|t|$.

Thus the range of nearly intrinsic behavior is pushed out to much larger $|t|$. In addition, there is a range of $t > 0$ which could be mistaken for intrinsic behavior,

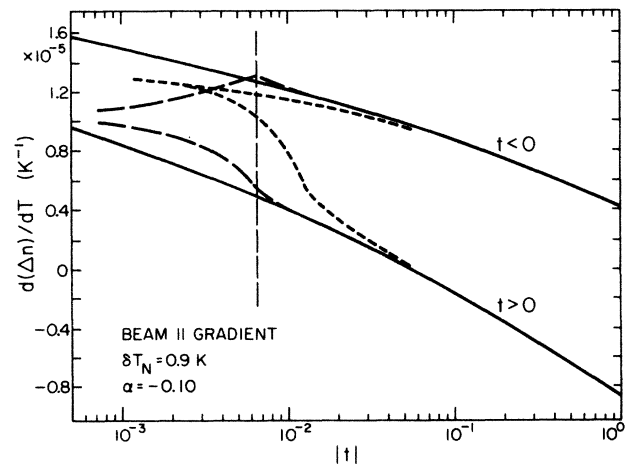


FIG. 4. Simulated data of $d(\Delta n)/dT$ vs $\log |t|$, as for Fig. 1, for the beam parallel to the gradient with $\delta T_N = 0.9$ K and $\alpha = -0.10$. The long-dashed lines indicate the behavior to be expected if the transition temperature is chosen to be at \bar{T}_N [i.e., $t = (T - \bar{T}_N)/\bar{T}_N$]. The short-dashed lines indicate the behavior corresponding to having chosen the transition temperature to be at the *peak* of $d(\Delta n)/dT$ in Fig. 1 [i.e., $t = (T - T_a)/T_a$]. The critical behavior in the absence of a gradient is indicated by the solid lines. The vertical line indicates the boundary of the gradient region. Note that the departure from the solid lines are more pronounced outside the gradient region if the transition temperature is chosen to be T_a rather than \bar{T}_N .

especially in the presence of the inevitable experimental noise and, if included in the analysis, would lead to grossly incorrect values of α . We see, then, that an accurate identification of \bar{T}_N is essential to restrict the departure of the data from the intrinsic behavior to the smallest possible range of $|t|$.

There is a lesson to be learned from these two experiments and their simulations. In the presence of a concentration gradient, the actual \bar{T}_N to be associated with an asymmetric peak in $C(T)$ is displaced somewhat toward the steep side of the apparent peak. This is so whether the true singularity is a cusp or a divergence. For the linear gradient case, \bar{T}_N actually lies in the center of a region of negative curvature.

Why is this of any special importance? If one assumes the peak of the data rounded by a concentration gradient to be \bar{T}_N , one makes an error of about $\frac{1}{2}\delta T_N$ in \bar{T}_N . This may not be of much consequence in, for instance, a measurement of the shift of T_N with applied magnetic field, provided the peak maintains the same shape; however, if the peak changes shape, as it does at $d=3$ in the crossover from REIM to random-field Ising model (RFIM) critical behavior,⁹ the error incurred can be quite serious. In the RFIM case, C_m and related functions, such as thermal expansion, exhibit a symmetric, logarithmic divergence at the phase transition T_c .⁹ It is readily demonstrated (and obvious) that a symmetric function rounded by any symmetric gradient effect will still have a peak at \bar{T}_c . Thus no error would be made when judging what the shift in T_c should be in the RFIM region. But the error made in determining \bar{T}_N in the REIM region would change the apparent origin of the RFIM shift, $T_c(H) - T_N \propto H^{2/\Phi}$, and would thereby affect the value obtained for the crossover exponent ϕ .

We believe that exactly this mistake has been made in the interpretation of the thermal expansion (dl/dT) on $\text{Mn}_{0.75}\text{Zn}_{0.25}\text{F}_2$ by Shapira *et al.*⁵ They chose the transition temperature to be at the peak of the dl/dT data for both $H=0$, where the peak is clearly asymmetric, and for $H>0$, where the peak is symmetric. Their analysis based on these measurements gave an exponent $\phi=1.24\pm 0.04$, which is equal to the susceptibility exponent γ of the *pure* Ising model (within experimental error). Because of this, Shapira *et al.* interpreted their result as indicative of crossover to RFIM behavior from *pure* Ising, *not* from REIM behavior.⁵ However, neutron-scattering results on the very same sample clearly yield REIM and *not* pure Ising results for the other critical (ν, γ) exponents.¹¹ Furthermore, all of the exponents measured at $x<0.9$ in the $\text{Fe}_x\text{Zn}_{1-x}\text{Fe}_2$ system also yield REIM results.^{12,13} We believe the dilemma can be resolved by simply choosing \bar{T}_N according to the results of the preceding section. This yields a value of \bar{T}_N approximately 0.070 K higher than the value at the peak in $H=0$. We then find the resulting ϕ to be very close to the expected¹⁴ and measured¹² REIM value of $\phi \simeq 1.4$. This is in keeping with Aharony's prediction¹⁴ that for the REIM to RFIM crossover $\Phi > \gamma$ (REIM)=1.31.

B. Neutron scattering

The neutron-scattering technique can provide a wealth of information for the characterization of phase transitions in magnetic crystals. However, unlike the direct measurement of the magnetic specific heat C , the process through which the extraction of critical exponents and amplitudes from the scattering data is made is considerably more indirect. It requires, first, an extensive analysis of the scattering intensity line shapes at a fixed reduced temperature $t=(T/T_c-1)$ and, second, determining how the parameters that characterize the line profile vary with t . Even in the pure $d=3$ Ising antiferromagnet FeF_2 (Ref. 15) the analysis of the quasielastic scattering data is nontrivial, since substantial corrections must be made for the spectrometer resolution. The interpretations of recent REIM (Ref. 12) and RFIM (Ref. 16) studies in dilute magnetic systems such as $\text{Fe}_x\text{Zn}_{1-x}\text{Fe}_2$ have additional uncertainty as to the proper theoretical forms for $S(\mathbf{q})$, the Fourier transform of the spin-spin correlation function to which the scattering intensity $I(\mathbf{q})$, after proper corrections for instrumental resolution, is proportional; \mathbf{q} is the reduced momentum transfer.¹⁷ Superimposed on all of the above is the complication that arises from the spread in transition temperatures induced by the concentration gradient in crystals of diluted magnetic systems. This is a particularly severe problem in quasielastic scattering experiments since large samples, (typically at least a few millimeters in each dimension), are required for adequate scattering intensity. The degree to which experimental results are affected by a spread in concentration has not been fully appreciated. In part, this is a consequence of having the magnitude of the gradients, when deduced from the critical scattering data directly, often underestimated. In addition, there has been a lack of understanding of how the data analysis is affected by the presence of the gradients.

Because of the importance of properly characterizing the REIM and RFIM critical behavior in diluted magnetic systems, we address the above issues by using computer simulations¹⁸ to make comparison with real experimental data. For purposes of simulation we use the Lorentzian form for $S(\mathbf{q})$ obtained from the Ornstein-Zernike approximation¹⁹

$$S(\mathbf{q}) = \frac{A}{q^2 + \kappa^2} \quad \text{for } \mathbf{q} \neq 0, \quad (6)$$

where $\kappa=1/\xi$ is the inverse correlation length. In the critical region κ behaves as

$$\kappa = \kappa_0^\pm |t|^\nu, \quad (7)$$

where ν is a positive exponent and κ_0^+ (κ_0^-) is the amplitude for $T > T_c$ ($T < T_c$).

The Lorentzian form for $S(\mathbf{q})$ is a reasonably good approximation for the pure Ising antiferromagnet FeF_2 ,¹⁵ although deviations from it are observable for $|t| \leq 10^{-3}$. Recent experiments¹² on a very homogeneous sample $\text{Fe}_{0.46}\text{Zn}_{0.54}\text{F}_2$ show that a Lorentzian $S(\mathbf{q})$ also works quite well at $H=0$ (REIM), despite theoret-

cal expectations of non-Lorentzian contributions.²⁰ [For $H \neq 0$ (RFIM), it has been shown experimentally¹⁶ that Eq. (6) is not at all adequate and a better approximation is to include an additional squared Lorentzian term.]

The effects that concentration gradients have on the interpretation of neutron-scattering-determined critical behavior are quite involved. The gradients enter $S(\mathbf{q})$ through the x dependence of the transition temperature $T_c(x)$; hence one can think of $S(\mathbf{q})$ as $S(\mathbf{q}, x)$. In the $\text{Fe}_x\text{Zn}_{1-x}\text{F}_2$ system $T_N(x)$ decreases nearly linearly with

x for $1 \geq x \geq 0.3$, i.e., $T_N(x) = xT_N(1)$.² Unlike the case of the specific heat, the averaging of $S(\mathbf{q}, x)$ over the sample is nontrivial in that $T_c(x)$ enters via the power-law dependence of κ , which appears in the denominator of Eq. (6). Furthermore, to relate the observed scattering intensity $I(\mathbf{q})$ to the correlation function $S(\mathbf{q}, x)$, a substantial correction must be made for the spectrometer resolution. The observed intensity for a transverse q scan is, to a good approximation,

$$I(q) = (I_0/V) \int_{\text{vol}} \int_{-\infty}^{\infty} \int_{-\infty}^{\infty} \int_{-\infty}^{\infty} S[(q-a), b, c, x] T(a) L(b) V(c) da db dc dV, \quad (8)$$

where $T(a)$, $L(b)$, and $V(c)$ are normalized resolution functions for the transverse, longitudinal, and vertical directions, respectively, and the spatially-dependent concentration x is accounted for by integrating over the sample volume V .

It is clear from Eq. (8) that the resolution correction to the observed $I(\mathbf{q})$ is quite dependent upon both the assumed form of $S(\mathbf{q})$ and the variation in x through the sample. Considering the complexity that Eq. (8) could take for arbitrary concentration gradients, it would be virtually impossible to deconvolve the effects of, say, non-Lorentzian contributions to $S(\mathbf{q})$ from those caused by the concentration gradient itself—unless one had an independent determination of the latter. The only truly reliable path to follow is to obtain crystals which are known to be so homogeneous that the critical behavior measurements are certain to be unaffected *above* some specified reduced temperature $|t|$.

The simulations we describe below provide insight as to how small the gradients must be to ensure that reliable critical behavior results can be obtained. The simulation involves using the initial parameters A , ν , κ_0^+ , and κ_0^- to create a series of q scans for T near T_N using Eq. (8), including a predetermined concentration gradient. The resulting simulated data are analyzed in precisely the same manner as real experimental scattering data by fitting them to the single Lorentzian line shape of Eq. (6) with the appropriate resolution corrections, and then determining the effective κ . This is repeated for a series of temperatures in the vicinity of T_N . A power-law fit of the resulting κ versus $|t|$ can then be made to determine the exponent ν .

To demonstrate the effect of a concentration gradient in the temperature dependence of $S(q)$ near the critical temperature, we choose to simulate the *pure* $d=3$ Ising model where ν , κ_0^+ , and κ_0^- are known, both from theory and experiment: $\nu=0.63$, $\kappa_0^+=0.45$ reciprocal-lattice units (rlu), and $\kappa_0^+/\kappa_0^- \approx 2$.¹⁵ Since the effects of longitudinal and vertical resolution are qualitatively similar, we need only transverse and vertical resolution functions in the form of Gaussians, which we choose to have half-widths at half maxima (HWHM) of 0.0017 and 0.042 rlu, respectively. (These are characteristic of the resolution functions in real scattering experiments on good-quality single crystals.) The resolution corrections were made

numerically, representing each Gaussian by 11 evenly spaced points q . The transverse scans were limited to the range $0.005 < |q| < 0.5$, with 42 points more densely spaced at smaller $|q|$, as is typical for experimental scans. (Note that no Bragg-scattering component enters into either the experiment or the simulation when q is restricted to $|q| > 0.005$, since this is much larger than the transverse HWHM of 0.0017.) We simulated results for a cylindrical sample with a linear concentration gradient along the axis, having a total variation of δx . This was done by considering the sample to be divided into 125 sections with x , and therefore $T_N(x)$, increasing linearly with position. The quantity $\Delta = \delta x / \bar{x} = \delta T_N / \bar{T}_N$ is the only relevant parameter in the summation, where \bar{x} and \bar{T}_N are the sample's average concentration and average transition temperature, respectively. $I_0 A$ was set equal to unity, giving intensities typical of real experiments. Gaussian noise was added to simulate the purely statistical noise in $I(\mathbf{q})$ observed in real experimental data.

Figure 5 shows the results of the analysis of the simulated data for $\Delta=0$, i.e., no gradient. As expected the values for κ agree with the power-law behavior shown by the solid curves over the entire range of $|t|$.

In Fig. 6 the effective κ obtained from the best fits to data with $\Delta=0.002$ is shown over the range $|t| < 0.005$. In this case we see an obvious departure from the intrinsic power-law behavior (shown by the solid curve) for $|t| < \Delta$, with a clear minimum occurring in the effective κ near $t=0$. Simulations for other values of Δ are consistent with this and indicate the general behavior that important deviations from the correct power-law behavior occur for $|t| \lesssim \Delta$ and that the effective κ flattens out at a nonzero value for $|t| \lesssim \Delta/2$. If one attempts to fit this data, excluding only the region of obvious rounding, one can be seriously misled by the apparent quality of the fit. Consider, for example, the fit to the simulated values of κ in Fig. 6, over the range $0.0007 \leq |t| \leq 0.01$. With an exponent $\nu=0.77$, an apparently reasonable fit is obtained (dashed curve in Fig. 6). This serious disagreement between this "effective" ν and the intrinsic $\nu=0.63$ indicates that one should be much more cautious in fitting data near the minimum in κ , and that a much wider range of $|t|$ should be excluded from the fits.

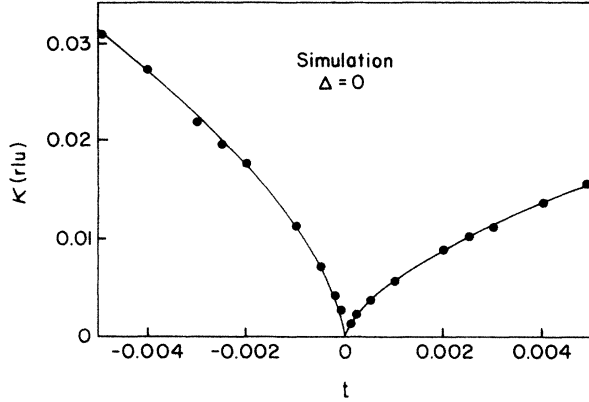


FIG. 5. Simulations of κ vs t (shown as dots) obtained by analyzing the simulated quasielastic-neutron-scattering line shapes in the vicinity of the phase transition with parameters appropriate to the pure $d=3$ Ising model. The simulation includes the effects of instrumental resolution and statistical noise as described in the text. The agreement with the solid line which is the power law ($\kappa = \kappa_0^\pm |t|^\nu$) used to generate the "data" is seen to be excellent.

In order to demonstrate that the increase in the effective ν is symptomatic of the effects of concentration gradients, we fit κ to power-law behavior for $|t|_{\min} \leq |t| \leq 0.05$ for two cases: $\Delta=0$ and $\Delta=0.002$. The ratio of the effective exponents $\nu(0.002)/\nu(0)$ is shown in Fig. 7 as a function of $|t|_{\min}$. For $|t|_{\min} \geq 0.002$ the ratio is unity within the error bars. This is consistent with the observation that the simulated κ agrees with the intrinsic power-law behavior for $|t| > \Delta$. As $|t|_{\min}$ becomes smaller the ratio systematically increases.

To see the manifestation of the effects indicated by the simulations above in real systems, we turn to the randomly diluted antiferromagnets for which the REIM ($H=0$) applies. In this instance the exponents are known theoretically with some accuracy but the amplitude ratios and $S(q)$ are not. [In the RFIM ($H \neq 0$) case

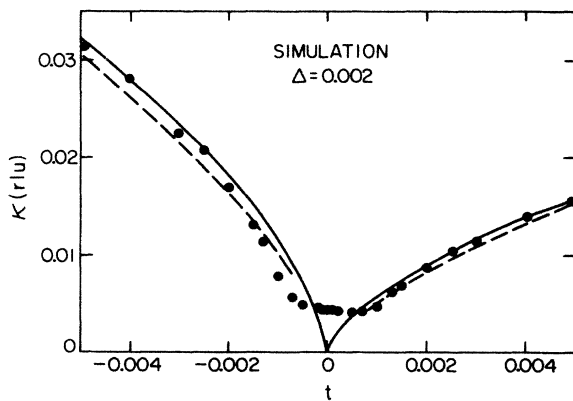


FIG. 6. Simulations of κ vs t , as in Fig. 5, for the hypothetical case of $\Delta = \delta T_N / \bar{T}_N = 0.002$, shown as the dots. Significant deviation of κ from the intrinsic power-law behavior (shown as the solid line) occurs for $|t| < \Delta$. For $|t| < \Delta/2$, κ is at its minimum value. The best fit over the range $0.0007 \leq |t| \leq 0.05$ is shown by dashed line, and is discussed in the text.

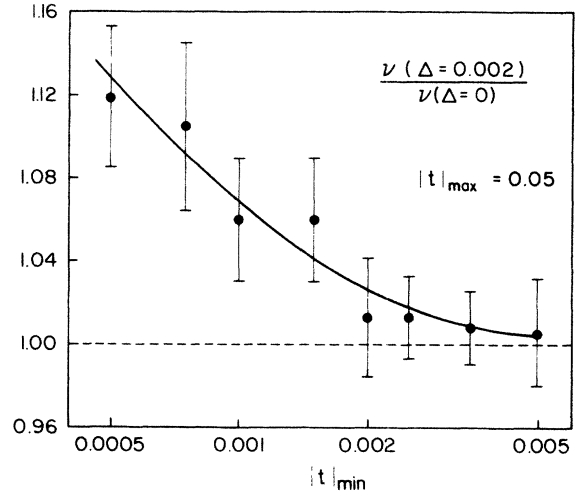


FIG. 7. Ratio of effective exponents $\nu(\Delta=0.002)/\nu(\Delta=0)$ obtained in power-law fits $\kappa = \kappa_0^\pm |t|^\nu$ as a function of the minimum value of reduced temperature $|t|_{\min}$ used in the analysis, for two simulations with $\Delta=0$ and $\Delta=0.002$, for a fixed $|t|_{\max} = 0.05$. Note that increasing error in $\nu(\Delta=0.002)/\nu(\Delta=0)$ occurs with decreasing choice of $|t|_{\min}$, for $|t|_{\min} \lesssim \Delta = 0.002$, while very little error occurs for $|t|_{\min} > \Delta$ (ratio $\rightarrow 1.0$). This error is entirely due to the error in $\nu(\Delta=0.002)$.

even less is known about the critical behavior.] We chose to demonstrate the effects of gradients by comparing the neutron-scattering results on two crystals of $\text{Fe}_x\text{Zn}_{1-x}\text{F}_2$ for which the measured gradients differ by more than an order of magnitude. One²¹ is a crystal of $\text{Fe}_{0.5}\text{Zn}_{0.5}\text{F}_2$, where the variation in x over the part of the sample used for neutron scattering was subsequently determined to be of order $\delta x \approx 0.01$ (see Fig. 8), and the

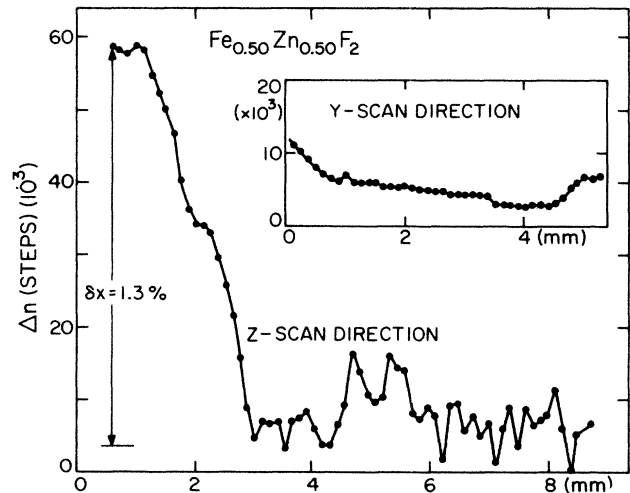


FIG. 8. The measured concentration gradient parallel (z scan) and perpendicular (y scan) to the crystal-growth direction of the $\text{Fe}_{0.5}\text{Zn}_{0.5}\text{F}_2$ sample used in the first neutron-scattering experiment (Ref. 23) on the REIM critical behavior. Although only 2 mm of the crystal was exposed to the neutron beam, it was unfortunately that portion with the maximum gradient. Hence for that experiment Δ could have been as large as $\Delta = \delta x / \bar{x} = 0.02$.

other¹² is a crystal of $\text{Fe}_{0.46}\text{Zn}_{0.54}\text{F}_2$ where $\delta x \approx 0.0002$ (see Fig. 7 of I). In both cases the concentration gradients were measured using the room-temperature birefringence technique described in I.

For the higher quality sample, $\text{Fe}_{0.46}\text{Zn}_{0.54}\text{F}_2$, the values obtained for κ using a Lorentzian line-shape analysis¹² follow the best-fit power-law behavior over the range $10^{-3} < |t| < 10^{-1}$ as shown in Fig. 9. From the simulation results just described we would expect deviations from power-law behavior only for $|t| < 0.0004$: hence the exponent ν and amplitudes κ_0^+ and κ_0^- obtained over the range $10^{-3} < |t| < 10^{-1}$ should accurately represent the intrinsic critical behavior.

In contrast, the $\text{Fe}_{0.5}\text{Zn}_{0.5}\text{F}_2$ sample shows a strong departure from apparent power-law behavior for $|t| \leq 3 \times 10^{-3}$, as is seen in Fig. 10. The intrinsically sharp REIM phase transition is obscured by the effects of the gradient. [In the case of a $d=3$ RFIM ($H \neq 0$) system such behavior in the very same sample has been incorrectly interpreted as evidence for the destruction of the phase transition.²²]

The agreement between the effective κ and the best fit appears to be quite good, possibly better than that between the best fit and the simulated data in Fig. 6. Nevertheless, these fits, over the range $5 \times 10^{-3} \leq |t| < 10^{-1}$ (not for $2 \times 10^{-3} < |t| < 10^{-1}$ as was incorrectly stated in Ref. 21), exclude data for t only in the region of $\kappa \approx \text{const}$ near $|t| \sim 0$, as was done in the simulation. It is therefore reasonable to expect that the effective exponents thus obtained should deviate from the intrinsic ones in the same direction as was found in the simulation.

This is indeed the case, as is seen from a comparison of the parameters obtained for this lower quality sample (*A*) and those obtained for the much higher quality $\text{Fe}_{0.46}\text{Zn}_{0.54}\text{F}_2$ one (*B*). Since the Fe concentrations of the two are almost the same, and both should represent the REIM universality class, ν and κ_0^+/κ_0^- should be

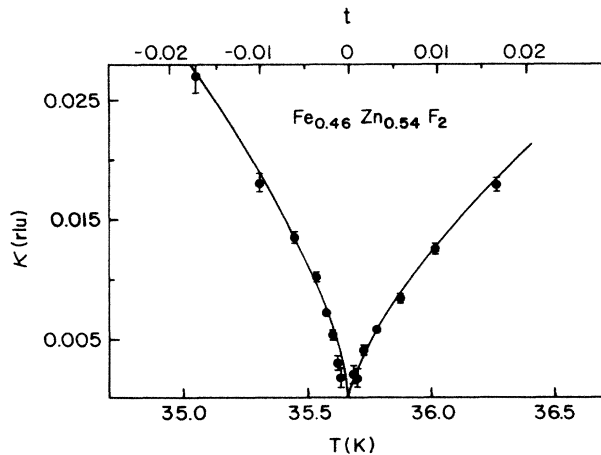


FIG. 9. κ vs T from the results (Ref. 12) of an analysis of the neutron-scattering line shapes in the very homogeneous sample ($\Delta=0.0004$) $\text{Fe}_{0.46}\text{Zn}_{0.54}\text{F}_2$. The solid curve is the best fit to the data for $0.001 \leq |t| \leq 0.1$ using the power law in Eq. (7). The excellent agreement even very close to T_c indicates that the fit reliably reflects the intrinsic critical behavior.

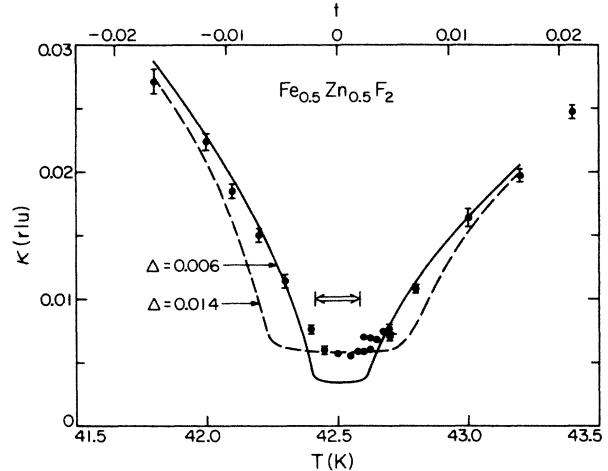


FIG. 10. Experimental points and simulations of the κ -vs- T results of the neutron-scattering experiment of Ref. 21. The solid and dashed curves are drawn for values of an assumed magnitude of a linear concentration gradient Δ as indicated, the choice for which is discussed in text. The inability to reproduce the experimental results is indicative of a nonlinear concentration gradient. The doubled-arrowed region is the span of temperature excluded from the original analysis (Ref. 21).

identical for the two crystals. Instead, we see that ν in crystal *A* is indeed higher ($\nu=0.73 \pm 0.02$) (Ref. 21) than it is in crystal *B* ($\nu=0.69 \pm 0.01$) (Ref. 12). This is precisely what one expects as has been demonstrated in Fig. 7. Hence we conclude that the higher value of ν obtained using crystal *A* (Ref. 21) reflects the larger spread in concentration in this sample. Clearly the value for ν obtained in sample *B*, where $\Delta \approx 0.0004$, more accurately represents the intrinsic REIM critical behavior. Moreover, it is in better agreement with theoretical predictions, namely, $\nu=0.70$ (Ref. 23) and 0.68 (Ref. 24). The observed ratio κ_0^+/κ_0^- also differs in the two crystals,^{12,21} which again is a direct consequence of the larger gradient in sample *A*.

In the same manner in which we analyzed the Δn data where the gradient was known, we have attempted to fit the neutron-scattering results on $\text{Fe}_{0.5}\text{Zn}_{0.5}\text{F}_2$. Two problems immediately arise. First, when we measure the concentration gradient, using the method described in I, we find the variation to be far from linear (see Fig. 8). Secondly, we do not know the exact location of the region of the crystal exposed to the neutron beam.

Despite these shortcomings, we have tried to approximate the effects of a gradient-rounded transition by a simulation in which we assume a linear gradient whose magnitude we adjust with the expectation of finding a best fit over the entire critical region. For the simulation we choose the values $\nu=0.69$ and $\kappa_0^+/\kappa_0^- = 0.69$ obtained from the analysis of the $\text{Fe}_{0.46}\text{Zn}_{0.54}\text{F}_2$ data discussed above. κ_0 is adjusted so as to provide an accurate fit for large $|t|$. We use Gaussian resolution line shapes with half widths corresponding to values actually measured in the $\text{Fe}_{0.5}\text{Zn}_{0.5}\text{F}_2$ experiment.

The results were most discouraging, as is seen in Fig.

10. We show the simulation for two values of Δ : $\Delta=0.014$ and 0.006 . The first was chosen so as to reproduce the experimentally observed minimum value of κ at $T=T_N$. However, the width of the region of nearly temperature independent κ is seen to be much broader than the experimental results would allow. If, instead, one judges the width of the broadened region to occur at the point where the experimental results first depart from power-law behavior (i.e., $\Delta=0$) and subsequently become almost temperature independent, then a value of $\Delta=0.006$ is obtained. But for this choice of Δ the minimum value of κ is 40% too low (choosing any smaller value might slightly improve agreement between experiment and simulation away from T_N but it does so at the expense of making the minimum κ even smaller). Our analysis strongly indicates no assumed value of linear concentration gradient can reproduce the observed κ -versus- T results; therefore, the *gradient cannot be linear*. The simulation results are not particularly sensitive to the resolution parameters used, nor are they affected much by the replacement of the nearly Gaussian vertical resolution by a triangular one, an approximation used in the original $\text{Fe}_{0.5}\text{Zn}_{0.5}\text{F}_2$ data analysis.²¹ Considerations related to more complex gradient distributions are discussed in Sec. V.

The fact that *no* choice of an assumed linear concentration gradient can reproduce the experimental results is indicative of the dangers in trying to judge the nature and extent of the gradient-induced rounding of the phase transition using only neutron scattering. The original estimate²¹ of the extent of the rounding in the exposed part of the $\text{Fe}_{0.5}\text{Zn}_{0.5}\text{F}_2$ crystal is indicated in Fig. 10. It corresponds to a reduced-temperature region $|t| \lesssim 2 \times 10^{-3}$. It is clear from our analysis that this was a unduly optimistic assessment. Had the authors²¹ had an independent measure of the concentration gradient, they would assuredly have been more reluctant to extend their data analysis to include measurements much below $|t| \approx 10^{-2}$. But, unaware of the shortcomings of the neutron-scattering technique in this regard, others have recently stated¹¹ in a study of REIM neutron scattering that “the measurements are limited by macroscopic, nonstatistical concentration fluctuations; *these are best characterized by the sharpness of the phase transition itself*” (italics added). The results on the $\text{Fe}_{0.5}\text{Zn}_{0.5}\text{F}_2$ sample indicate that this is *not* the case; this technique yields gradient rounding estimates which are consistently too small.

We have shown that excluding only the region of obvious rounding from analysis of the data leads to values of ν which are too large. Nevertheless, this criterion is routinely used:¹¹ “the overall spread in concentration being less than 0.1%; we have therefore performed measurements down to $\sim 4 \times 10^{-4}$ in reduced temperature.” A similar error has apparently been made in the analysis of a RFIM experiment in the weakly anisotropic system $\text{Mn}_x\text{Zn}_{1-x}\text{F}_2$.²² A minimum in κ versus t has been observed, and a gradient-induced rounding of the transition is inferred. (We believe the rounding to be underestimated by a factor of 2, based on the results of the present simulations.) A power-law fit of κ versus $|t|$ is

made, in which T_c is arbitrarily chosen to be far below the region of the minimum in κ as seen in their Fig. 4,¹¹ and indeed, below the range of rounding of the transition. By doing this a value of $\nu=1.52 \pm 0.13$ is obtained. If, however, the region of rounding is eliminated from consideration and T_c is assumed to be near the minimum in κ , the result for the RFIM exponent ν agrees with that obtained in the strongly anisotropic system $\text{Fe}_{0.46}\text{Zn}_{0.54}\text{F}_2$, namely $\nu=1.0 \pm 0.15$.¹⁶

Even the qualitative effect of a concentration gradient on the shape of the measured κ versus t is not immediately obvious from the neutron-scattering data alone. Thus one finds claims in the literature such as “More importantly, the data also depart from linearity as $T_N(H)$ is approached. This is *not* due to sample inhomogeneities; it may readily be seen that in a neutron experiment in which the entire profile is fitted, a *distribution of T_N 's causes κ to be depressed rather than increased.*”²² (italics added). Our analysis above show the exact opposite to be the case.

IV. CONSIDERATIONS OF THE EFFECTS OF MORE COMPLEX GRADIENTS

The linear variation of concentration with position discussed thus far is a somewhat arbitrary idealization of what actually occurs in the crystal-growth process. Any other variation would modify the shape of the rounding behavior to be expected for the specific heat or neutron-scattering critical behavior, through the distribution function of concentration $W(x)$. We briefly examine several more complicated variations and the distribution functions $W(x)$ corresponding to them. These are shown in Fig. 11, which though idealizations themselves, are representative of cases that have actually been observed (see I). Figure 11(a) illustrates an inflection in concentration superimposed on a linear gradient that might originate from a temperature variation in the growth process. A quasiperiodic series of these often arises (see Fig. 2) because of the constitutional supercooling instability. Figure 11(b) illustrates a reversal of gradient, such as the one responsible for the “super” $\text{Fe}_{0.46}\text{Zn}_{0.54}\text{F}_2$ sample. We do not understand the underlying mechanism which produces this effect. Figure 11(c) illustrates a random variation which might be caused by a very noisy or unstable temperature control. Figure 11(d) illustrates periodic variations induced by stirring of the melt during growth via the accelerated crucible rotation technique (see discussion in I).

In view of the involved analysis already required to interpret the critical behavior associated with the neutron-scattering experiments, even for the relatively simple linear gradient case, one cannot help but surmise that the interpretation would be made considerably more complex in the presence of any one of the four forms for $W(x)$ shown in Fig. 11. Choosing \bar{T}_N and the region of reduced temperature beyond which it was meaningful to retain data for the analysis would become increasingly difficult to judge—and still more so if the unknown $W(x)$ was not symmetric. Needless to say, it would be virtually impossible to invert the process, that is, deter-

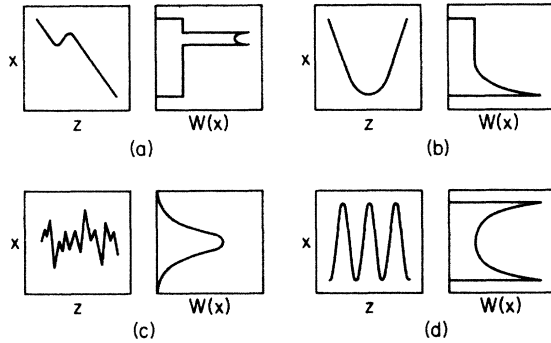


FIG. 11. Schematic variation of concentration x with position z in crystal and the distribution function $W(x)$ vs x for (a) nearly linear gradient, (b) reversal of gradient, (c) random variation with Gaussian distribution induced by noisy temperature control in the growth process, and (d) sinusoidal variation induced by accelerated crucible rotation technique (see I). In the case of $\text{Fe}_x\text{Zn}_{1-x}\text{F}_2$, where $T_N(x) = xT_N(1)$ for $0.3 \leq x \leq 1$, $W(x) \propto W(T_N)$, the distribution function of Néel temperatures.

mine $W(x)$ from the critical behavior observed in the neutron-scattering case, although it is precisely this that has been claimed to have been done by Birgeneau *et al.*^{11,21}

V. CONCLUSIONS

Given the variety of different gradient effects which have been observed, we see that it is extremely desirable

to have a microscopic method of analysis of the actual sample to be used in critical phenomena experiments, both to establish the concentration inhomogeneities, and to choose the best region within a given sample. It is not sufficient to have a bulk analysis, either of the actual sample, or of both ends of the boule, since this is not sensitive either to short-range fluctuations, or to an effect such as a gradient reversal.

Once having determined the gradient and assuming it to be small enough so as to not cause rounding through most of the critical region, it then is necessary to include only that data which lies well outside the region of rounding. However, the most desirable circumstance is obtained when one chooses a crystal with the smallest possible concentration gradient, as is the case for the "super" $\text{Fe}_{0.46}\text{Zn}_{0.54}\text{F}_2$ crystal.

ACKNOWLEDGMENTS

We are indebted to N. Nighman for having grown all of the crystals used in this study. The research at University of California, Santa Barbara (UCSB) has been supported by National Science Foundation Grants No. DMR-80-17582 and No. DMR-85-16786. One of us (D.P.B.) gratefully acknowledges support from the University of California, Santa Cruz (UCSC) Committee on Research and the Junior Faculty Fellowship Committee.

- ¹A. R. King, I. B. Ferreira, V. Jaccarino, and D. P. Belanger, preceding paper, *Phys. Rev. B* **37**, 219 (1988).
- ²G. K. Wertheim, D. N. E. Buchanan, and H. J. Guggenheim, *Phys. Rev.* **152**, 527 (1966).
- ³P. Wong, S. von Molnar, and P. Dimon, *Solid State Commun.* **48**, 573 (1983).
- ⁴R. J. Birgeneau, R. A. Cowley, G. Shirane, and H. Yoshizawa, *Phys. Rev. Lett.* **54**, 2147 (1985).
- ⁵Y. Shapira, N. F. Olivera, Jr., and S. Foner, *Phys. Rev. B* **30**, 6639 (1984).
- ⁶M. Fähnle, *J. Magn. Magn. Mater.* **59**, 266 (1986); see references to other theoretical works on phase transitions in macroscopically inhomogeneous systems contained therein.
- ⁷A. B. Harris, *J. Phys. C* **7**, 1671 (1974).
- ⁸D. P. Belanger, A. R. King, and V. Jaccarino, *Phys. Rev. B* **29**, 2636 (1984).
- ⁹D. P. Belanger, A. R. King, V. Jaccarino, and J. L. Cardy, *Phys. Rev. B* **28**, 2522 (1983).
- ¹⁰I. B. Ferreira, A. R. King, V. Jaccarino, J. L. Cardy, and H. J. Guggenheim, *Phys. Rev. B* **28**, 5192 (1983).
- ¹¹P. W. Mitchell, R. A. Cowley, H. Yoshizawa, P. Boni, Y. Uemura, and R. J. Birgeneau, *Phys. Rev. B* **1**, 4719 (1986).
- ¹²See D. P. Belanger, A. R. King, and V. Jaccarino, *Phys. Rev. B* **34**, 452 (1986) for values of ν , γ , and α and the REIM \rightarrow RFIM crossover exponent ϕ .
- ¹³See P. Barrett, *Phys. Rev. B* **34**, 3513 (1986), for the value of β .
- ¹⁴A. Aharony, *Europhys. Lett.* **1**, 617 (1986).
- ¹⁵D. P. Belanger and H. Yoshizawa, *Phys. Rev. B* **35**, 4823 (1987).
- ¹⁶D. P. Belanger, A. R. King, and V. Jaccarino, *Phys. Rev. B*

31, 4538 (1985).

- ¹⁷See, for example, J. Als-Nielsen, *Phase Transitions and Critical Phenomena*, edited by C. Domb and M. S. Green (Academic, New York, 1976), Vol. 5A.
- ¹⁸Additional applications of simulation techniques to neutron scattering are given in D. P. Belanger, M. I. Setliff, and D. M. Stone (unpublished).
- ¹⁹See, for example, H. B. Tarko and M. E. Fisher, *Phys. Rev. B* **11**, 1217 (1975).
- ²⁰R. A. Pelcovits and A. Aharony, *Phys. Rev. B* **31**, 350 (1985).
- ²¹R. J. Birgeneau, R. A. Cowley, G. Shirane, H. Yoshizawa, D. P. Belanger, A. R. King, and V. Jaccarino, *Phys. Rev. B* **27**, 6747 (1983).
- ²²R. J. Birgeneau, Y. Shapira, G. Shirane, R. A. Cowley, and H. Yoshizawa, *Physica* **137B**, 83 (1986). These authors claim "the neutron data in both $\text{Fe}_x\text{Zn}_{1-x}\text{F}_2$ and $\text{Mn}_x\text{Zn}_{1-x}\text{F}_2$ show that there is no divergent antiferromagnetic length for either field cooling or zero-field cooling at any field, so that there can be no second-order transition in the antiferromagnetic order parameter." The statement is in contradiction with evidence from other scattering studies [D. P. Belanger, V. Jaccarino, A. R. King, and R. Nicklow, *Phys. Rev. Lett.* (to be published)]; Monte Carlo studies [A. T. Ogielski, *Phys. Rev. Lett.* **57**, 1251 (1986); A. T. Ogielski and D. A. Huse, *ibid.* **56**, 1298 (1986)]; and exact calculations for the $d=3$ RFIM Ising model [J. Z. Imbrie, *Phys. Rev. Lett.* **53**, 1747 (1984)].
- ²³K. E. Newman and E. K. Riedel, *Phys. Rev. B* **25**, 264 (1982).
- ²⁴G. Jug, *Phys. Rev. B* **27**, 609 (1983).